

# Deep sub-threshold $\phi$ production and implications for the $K^+/K^-$ freeze-out in Au+Au collisions

J. Adamczewski-Musch<sup>4</sup>, O. Arnold<sup>10,9</sup>, C. Behnke<sup>8</sup>, A. Belounnas<sup>15</sup>, A. Belyaev<sup>7</sup>, J.C. Berger-Chen<sup>10,9</sup>, J. Biernat<sup>3</sup>, A. Blanco<sup>2</sup>, C. Blume<sup>8</sup>, M. Böhmer<sup>10</sup>, P. Bordalo<sup>2</sup>, S. Chernenko<sup>7,†</sup>, L. Chlad<sup>16</sup>, C. Deveaux<sup>11</sup>, J. Dreyer<sup>6</sup>, A. Dybczak<sup>3</sup>, E. Epple<sup>10,9</sup>, L. Fabbietti<sup>10,9</sup>, O. Fateev<sup>7</sup>, P. Filip<sup>1</sup>, P. Fonte<sup>2,a</sup>, C. Franco<sup>2</sup>, J. Friese<sup>10</sup>, I. Fröhlich<sup>8</sup>, T. Galatyuk<sup>5,4</sup>, J. A. Garzón<sup>17</sup>, R. Gernhäuser<sup>10</sup>, M. Golubeva<sup>12</sup>, F. Guber<sup>12</sup>, M. Gumberidze<sup>5,b</sup>, S. Harabasz<sup>5,3</sup>, T. Heinz<sup>4</sup>, T. Hennino<sup>15</sup>, S. Hlavac<sup>1</sup>, C. Höhne<sup>11</sup>, R. Holzmann<sup>4</sup>, A. Ierusalimov<sup>7</sup>, A. Ivashkin<sup>12</sup>, B. Kämpfer<sup>6,c</sup>, T. Karavicheva<sup>12</sup>, B. Kardan<sup>8</sup>, I. Koenig<sup>4</sup>, W. Koenig<sup>4</sup>, B. W. Kolb<sup>4</sup>, G. Korcyl<sup>3</sup>, G. Kornakov<sup>5</sup>, R. Kotte<sup>6</sup>, W. Kühn<sup>11</sup>, A. Kugler<sup>16</sup>, T. Kunz<sup>10</sup>, A. Kurepin<sup>12</sup>, A. Kurilkin<sup>7</sup>, P. Kurilkin<sup>7</sup>, V. Ladygin<sup>7</sup>, R. Lalik<sup>10,9</sup>, K. Lapidus<sup>10,9</sup>, A. Lebedev<sup>13</sup>, L. Lopes<sup>2</sup>, M. Lorenz<sup>8,9</sup>, T. Mahmoud<sup>11</sup>, L. Maier<sup>10</sup>, A. Mangiarotti<sup>2</sup>, J. Markert<sup>4</sup>, S. Maurus<sup>10</sup>, V. Metag<sup>11</sup>, J. Michel<sup>8</sup>, D.M. Mihaylov<sup>10,9</sup>, S. Morozov<sup>12,d</sup>, C. Müntz<sup>8</sup>, R. Münzer<sup>10,9</sup>, L. Naumann<sup>6</sup>, K. N. Nowakowski<sup>3</sup>, M. Palka<sup>3</sup>, Y. Parpottas<sup>14,e</sup>, V. Pechenov<sup>4</sup>, O. Pechenova<sup>8</sup>, O. Petukhov<sup>12,d</sup>, J. Pietraszko<sup>4</sup>, W. Przygoda<sup>3</sup>, S. Ramos<sup>2</sup>, B. Ramstein<sup>15</sup>, A. Reshetin<sup>12</sup>, P. Rodriguez-Ramos<sup>16</sup>, P. Rosier<sup>15</sup>, A. Rost<sup>5</sup>, A. Sadovsky<sup>12</sup>, P. Salabura<sup>3</sup>, T. Scheib<sup>8</sup>, H. Schuldes<sup>8</sup>, E. Schwab<sup>4</sup>, F. Scozzi<sup>5,15</sup>, F. Seck<sup>5</sup>, P. Sellheim<sup>8</sup>, J. Siebenson<sup>10</sup>, L. Silva<sup>2</sup>, Yu.G. Sobolev<sup>16</sup>, S. Spataro<sup>f</sup>, H. Ströbele<sup>8</sup>, J. Stroth<sup>8,4</sup>, P. Strzemepek<sup>3</sup>, C. Sturm<sup>4</sup>, O. Svoboda<sup>16</sup>, P. Tlusty<sup>16</sup>, M. Traxler<sup>4</sup>, H. Tsertos<sup>14</sup>, E. Usenko<sup>12</sup>, V. Wagner<sup>16</sup>, C. Wendisch<sup>4</sup>, M.G. Wiebusch<sup>8</sup>, J. Wirth<sup>10,9</sup>, Y. Zanevsky<sup>7,†</sup>, P. Zumbrun<sup>4</sup>  
(HADES collaboration)

<sup>1</sup>*Institute of Physics, Slovak Academy of Sciences, 84228 Bratislava, Slovakia*

<sup>2</sup>*LIP-Laboratório de Instrumentação e Física Experimental de Partículas, 3004-516 Coimbra, Portugal*

<sup>3</sup>*Smoluchowski Institute of Physics, Jagiellonian University of Cracow, 30-059 Kraków, Poland*

<sup>4</sup>*GSI Helmholtzzentrum für Schwerionenforschung GmbH, 64291 Darmstadt, Germany*

<sup>5</sup>*Technische Universität Darmstadt, 64289 Darmstadt, Germany*

<sup>6</sup>*Institut für Strahlenphysik, Helmholtz-Zentrum Dresden-Rossendorf, 01314 Dresden, Germany*

<sup>7</sup>*Joint Institute of Nuclear Research, 141980 Dubna, Russia*

<sup>8</sup>*Institut für Kernphysik, Goethe-Universität, 60438 Frankfurt, Germany*

<sup>9</sup>*Excellence Cluster 'Origin and Structure of the Universe', 85748 Garching, Germany*

<sup>10</sup>*Physik Department E62, Technische Universität München, 85748 Garching, Germany*

<sup>11</sup>*II. Physikalisches Institut, Justus Liebig Universität Giessen, 35392 Giessen, Germany*

<sup>12</sup>*Institute for Nuclear Research, Russian Academy of Science, 117312 Moscow, Russia*

<sup>13</sup>*Institute of Theoretical and Experimental Physics, 117218 Moscow, Russia*

<sup>14</sup>*Department of Physics, University of Cyprus, 1678 Nicosia, Cyprus*

<sup>15</sup>*Institut de Physique Nucléaire, CNRS-IN2P3, Univ. Paris-Sud, Université Paris-Saclay, F-91406 Orsay Cedex, France*

<sup>16</sup>*Nuclear Physics Institute, The Czech Academy of Sciences, 25068 Rez, Czech Republic*

<sup>17</sup>*LabCAF. F. Física, Univ. de Santiago de Compostela, 15706 Santiago de Compostela, Spain*

<sup>a</sup> also at ISEC Coimbra, Coimbra, Portugal

<sup>b</sup> also at ExtreMe Matter Institute EMMI, 64291 Darmstadt, Germany

<sup>c</sup> also at Technische Universität Dresden, 01062 Dresden, Germany

<sup>d</sup> also at Moscow Engineering Physics Institute (State University), 115409 Moscow, Russia

<sup>e</sup> also at Frederick University, 1036 Nicosia, Cyprus

<sup>f</sup> also at Dipartimento di Fisica and INFN, Università di Torino, 10125 Torino, Italy

<sup>g</sup> also at Utrecht University, 3584 CC Utrecht, The Netherlands

<sup>†</sup> deceased

(Dated: 23.03.2017)

We present first data on charged kaons and  $\phi$  mesons in Au+Au collisions at a kinetic beam energy of 1.23A GeV. As observed already at slightly higher beam energies, we find significantly different slopes for the  $K^+$  and  $K^-$  transverse-mass spectra, and no significant increase of the the  $K^-/K^+$  multiplicity ratio with increasing centrality of the collision. The  $\phi/K^-$  multiplicity ratio is found to be surprisingly high with a value of  $0.52 \pm 0.16$  and shows no dependence on the centrality, either. The different slopes of the  $K^+$  and  $K^-$  spectra can be explained by feed-down from  $\phi$  mesons, which substantially softens the spectra of  $K^-$  mesons.

PACS numbers:

The possible appearance of a  $\bar{K}$  condensate in dense nuclear matter has triggered extensive activities since it was proposed by Kaplan and Nelson [1]. Hadron properties at high baryo-chemical potential cannot be addressed directly by ab-initio QCD calculations and thus have to be modeled using effective Lagrangians. Various approaches [2–7] predict a net attractive  $\bar{K}$ -nucleon potential. However, due to the presence and properties of baryon resonances [8, 9], the  $\bar{K}$  spectral function has a complicated form, whose details differ between the different approaches.

The first high-quality data on sub-threshold  $K^-$  production in relativistic heavy-ion collisions (HIC) have become available in the late 1990s [10–12]. The data revealed a similar rise of  $K^+$  and  $K^-$  yields with increasing centrality of the collision, and systematically softer  $K^-$  spectra compared to the ones of the  $K^+$ . Detailed comparisons between data and transport models suggest that the  $K^-$  decouples from the system later than the  $K^+$  due to the large cross section of strangeness exchange reaction, e.g.  $\pi Y \rightarrow N\bar{K}$  which were predicted in [13], as the dominant source for sub-threshold  $K^-$  production. This would explain the softer spectra of the  $K^-$  (due to the later freeze-out) as well as the similar dependence on the system size (coupling of  $K^-$  yield to the one of the  $K^+$  via the hyperons) [14]. Attempting to extract the  $\bar{K}$ -N potential, most comparisons between  $K^-$  data and transport models seem to favor a somewhat attractive  $\bar{K}$ -N potential. However, quantitative conclusions remain vague and under discussion [15–17]. Nevertheless, a link to astrophysical objects has been established by connecting the effective reduction of the  $K^-$  mass and the appearance of  $K^-$  condensates in the interior of neutron stars [18], which was predicted to limit the maximum possible neutron star mass to 1.5 solar masses [19]. The recent discovery of neutron stars with masses close to 2 solar masses [20, 21] made this predicted constraint obsolete.

Recent data reveal that a sizable ( $\approx 20\%$ ) fraction of the observed  $K^-$  yield results from  $\phi$  decays in small collision system [22–26]. The  $\phi$  meson cross section is generally assumed to be small in a hadronic system due to the OZI suppression [27]. Consequently,  $\phi$  enhancement has been suggested as a signature for plasma formation [28] and the  $\phi$  contribution to the  $K^-$  multiplicity is assumed to be small or is even neglected in discussions on strangeness production at SIS energies based on hadronic transport models [14–17, 29]. Since the first discussion of  $\phi$  mesons as a possible source of  $K^-$  mesons at SIS energies [30], various explanations for the large  $\phi/K^-$  ratio in small systems have been put forward, based on both macroscopic [31, 32] and microscopic models [33, 34]. HADES has been able to show that the observed difference in the slope of the  $K^+$  and  $K^-$  spectra can be explained by taking the  $K^-$  contribution from  $\phi$  decays into account in light collision systems, as those  $K^-$  have a substantially softer spectrum [35], which was confirmed later [24–26]. In this letter, we present  $K^\pm$  and  $\phi$  data reconstructed

from Au+Au collisions at a kinetic beam energy of 1.23A GeV ( $\sqrt{s_{NN}} = 2.4$  GeV). In contrast to previous measurements, the mesons are produced much deeper below their corresponding free NN threshold with an excess-energy of -150 MeV ( $K^+$ ), -450 MeV ( $K^-$ ) and -490 MeV ( $\phi$ ). In addition, also the system size is increased. In the classical particle picture one expects the  $\phi/K^-$  to decrease when going down in energy, as it becomes increasingly unlikely to accumulate enough energy for  $\phi$  production while the  $K^-$  yield can still be fed from strangeness exchange reactions, which should have sufficient time to occur in such a large system. Therefore, this is an ideal environment to test the importance of resonant production vs. production via strangeness exchange of antikaons.

HADES is a charged-particle detector located at the GSI Helmholtz Center for Heavy Ion Research in Darmstadt, Germany. It comprises a 6-coil toroidal magnet centered around the beam axis and six identical detection sections located between the coils covering almost the full azimuthal angle. Each sector is equipped with a Ring-Imaging Cherenkov (RICH) detector followed by low-mass Mini-Drift Chambers (MDCs), two in front of and two behind the magnetic field, as well as a scintillator hodoscope (TOF) and a Resistive Plate Chamber (RPC). The RICH detector is used mainly for electron/positron identification, the MDCs are the tracking detectors, while the TOF and RPC are used for time-of-flight measurements in combination with a diamond start detector located in front of a 15-fold segmented target. The multiplicity trigger is based on the hit multiplicity in the TOF covering a polar angle range between  $45^\circ$  and  $85^\circ$ . A detailed description is given in [37].

In total  $2.1 \times 10^9$  Au+Au events have been collected corresponding to the 40% most central events estimated by elaborated studies using a Glauber model [38, 39]. Charged particle trajectories were reconstructed using the MDC information. The resulting tracks were subject to several selections based on quality parameters delivered by a Runge-Kutta track fitting algorithm. Particle identification is based on the measurements of time-of-flight and track length. Additional separation power for kaons is gained by the energy-loss information from the MDC and the TOF detectors.  $K^+$  mesons are identified in nine rapidity bins ranging from center of mass rapidity of  $y_{cm} = -0.65$  to  $y_{cm} = +0.25$  in steps of 0.1, and in up to seven transverse mass ( $m_t = \sqrt{p_t^2 + m_0^2}$ ) bins in steps of 25 MeV/ $c^2$ . The mass of the kaon candidates is calculated from their momentum and velocity. The distribution shows a peak at the nominal kaon mass. The underlying background is estimated in an iterative fitting procedure. The fit parameters are observed to show little and strictly monotonous increase with increasing momentum, exhibiting quantitative agreement with the Monte-Carlo simulation. This procedure allows to obtain the statistical error of the signal and to take into account the quality of the background description of the fit function. Additional variations of the number of pa-

rameters, the fit and the integration ranges turned out to be well covered by the error given by the fit. An example of a  $K^+$  signal and the corresponding background adaption is displayed in the upper inset of Fig. 1 for the region covering mid-rapidity and reduced transverse mass  $m_t - m_0$  between 25 and 50  $\text{MeV}/c^2$ .  $K^-$  are identified similarly as the  $K^+$  but in only four rapidity regions, ranging from  $y_{cm} = -0.7$  to  $+0.1$  in steps of 0.2 units in rapidity, and up to seven transverse mass bins in steps of 25  $\text{MeV}/c^2$ , due to the lower statistics compared to the  $K^+$ . An example of a  $K^-$  signal including the background fit is displayed in the middle inset of Fig. 1 for the region covering mid-rapidity and  $m_t - m_0$  between 50 and 75  $\text{MeV}/c^2$ .  $\phi$  mesons are identified via their decay into charged kaons. This analysis is done in three rapidity bins, ranging from  $y_{cm} = -0.5$  to  $+0.1$  in steps of 0.2 units in rapidity, and three transverse mass bins in steps of 100  $\text{MeV}/c^2$ . The combinatorial background is described with the mixed-event technique. For systematic error evaluation on the count rate, the normalization region of the mixed-event and the integration range are varied. The error of the extracted count rate is then defined in the same way as done for the kaons. An example of a  $\phi$  signal in the  $K^+K^-$  invariant mass after subtraction of the background is displayed on the lower inset of Fig. 1 for the mid-rapidity region and  $m_t - m_0$  between 0 and 100  $\text{MeV}/c^2$ .

The raw count rates are corrected in each phase space cell for acceptance and efficiency based on Monte-Carlo and Geant simulations, subject to the same reconstruction and analysis steps as the experimental data. The combined (inverse) correction factors for efficiency and acceptance correspond to  $\approx 0.2$  for kaons and about 0.04 for  $\phi$  mesons, for details see [41]. As input for the efficiency and acceptance simulation, thermally distributed  $K^+$  and  $\phi$  mesons with a temperature of 100 MeV and 80 MeV for the  $K^-$  are embedded into Au+Au collisions generated with the transport code UrQMD [40] serving as background events. The systematic bias and uncertainties of the correction are checked based on the more abundant proton and pion tracks as well as on the difference between the different sectors of HADES and are either corrected or taken into account as systematic error. The total systematic uncertainty on the charged kaon yields within the acceptance corresponds to 4%. The acceptance and efficiency corrected transverse mass spectra of  $K^\pm$  and  $\phi$  mesons for the mid-rapidity bin are presented in Fig. 1. The number of counts per event, per transverse mass and per unit in rapidity, divided by  $m_t^2$  are displayed. This representation is chosen to ease a comparison with Boltzmann fits to the resulting distribution according to

$$\frac{1}{m_t^2} \frac{d^2N}{dm_t dy_{cm}} = C(y_{cm}) \exp\left(-\frac{(m_t - m_0)}{T_B(y_{cm})}\right). \quad (1)$$

Using Eq. (1) for extrapolation in  $m_t - m_0$  and integrating the data points, the rapidity density distributions for the different particles are obtained, see Fig. 2. The

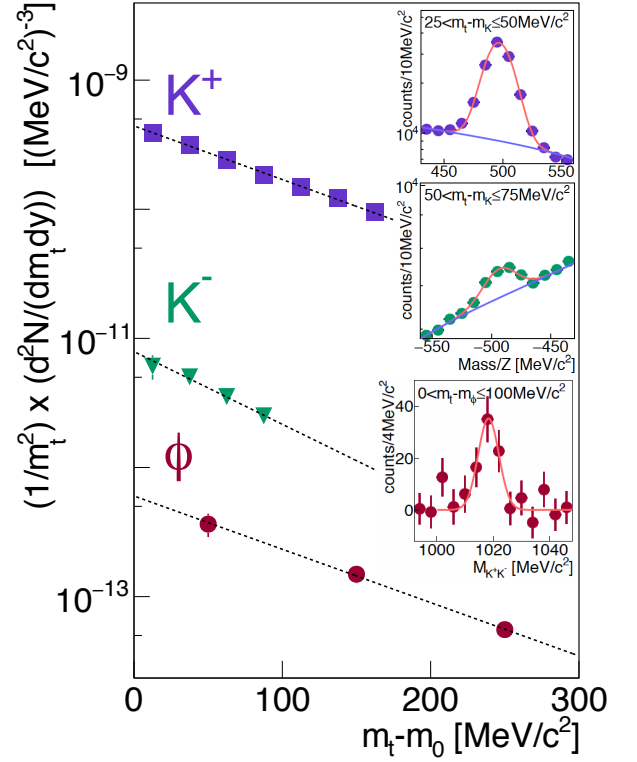


FIG. 1: Left: Acceptance and efficiency corrected transverse-mass spectra around mid-rapidity. The number of counts per event, per transverse mass and per rapidity region, divided by  $m_t^2$  together with a fit to the data points according to Eq. (1) for the 0-40% most central events is displayed. Upper right:  $K^+$  signal and the corresponding background fit for the region covering mid-rapidity and  $m_t - m_0$  between 25 and 50  $\text{MeV}/c^2$ . The red curve corresponds to the Gaussian part and the blue one to the polynomial part of the combined function used for signal extraction. Middle right: Same as upper one but for  $K^-$  and  $m_t - m_0$  between 50 and 75  $\text{MeV}/c^2$ . Lower right:  $K^+K^-$  invariant mass distribution for the mid-rapidity region and  $m_t - m_0$  between 0 and 100  $\text{MeV}/c^2$  after subtraction of the background.

uncertainty of the extrapolation is estimated to 1.5% from the difference between the extrapolation based on Eq. (1) and a Siemens-Rasmussen model function including a radial expansion velocity as parameter fixed by using the kinematic distribution of the protons in the same collision system [41]. Adding up the different errors quadratically, we find an overall systematic uncertainty on the yield within the covered rapidity range of  $\approx 5\%$  for charged kaons and of  $\approx 10\%$  for the  $\phi$ .

Multiplicities are obtained integrating over  $y_{cm}$  and using a Gaussian function for extrapolation to full phase space. The uncertainty of this extrapolation is estimated based on the relative fraction of extrapolated yield between the fitted Gaussian functions and the rapidity yield distributions obtained from UrQMD. The obtained total multiplicities are listed in Tab. I. The rapidity distributions and the Gaussian functions used for extrapolation in  $y_{cm}$  are displayed on the left

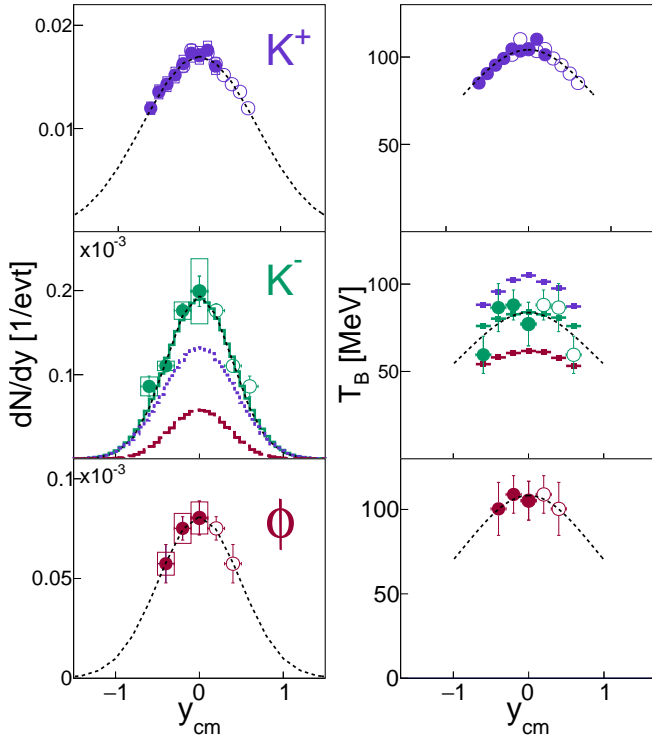


FIG. 2: Left: Rapidity distributions and the Gaussian functions (dashed curves) used for extrapolation in  $y_{cm}$  for the three mesons. Points reflected at mid-rapidity are displayed as open symbols. Right: Extracted inverse slope parameters obtained from the Boltzmann fits to the  $m_t$  spectra. The distributions are adapted using  $T_B = \frac{T_{eff}}{\cosh(y_{cm})}$ , displayed as dashed curve. Both figures show results for the 0-40% most central events. In case of the  $K^-$  also the yields and the extracted inverse slopes of the two-component model are displayed: Direct thermal (blue), resulting from  $\phi$  decays (red), sum of both (green), see text for details.

panel of Fig. 2 for the three mesons. The error bars display the statistical error, while the systematic error is indicated by the boxes. The extracted inverse slope parameters obtained from the Boltzmann fits to the  $m_t$  spectra are displayed on the right panel of Fig. 2. The dependence is fitted using  $T_B = \frac{T_{eff}}{\cosh(y_{cm})}$  in order to obtain the effective inverse slope  $T_{eff}$ . While  $T_{eff}$  is extracted to  $(104 \pm 1_{stat} \pm 1_{sys})$  MeV for  $K^+$  and to  $(108 \pm 7_{stat})$  MeV for  $\phi$  mesons, the obtained value for  $K^-$  of  $(84 \pm 6_{stat})$  MeV is significantly lower. This is in line with the previously obtained systematics [12]. The systematic error on the inverse slope of the  $K^+$  is obtained by comparison of the spectra extracted in the different sectors separately. In case of the  $K^-$  and  $\phi$  mesons, a similar check gives variations well below the statistical errors and hence are neglected. In addition, the analysis procedure is repeated in four and two centrality classes for the  $K^+$  and  $K^-$ ,  $\phi$ , respectively, which correspond to 10% (20%) steps in centrality. The results are summarized in Tab. I. Due to the reduced statistics, we take the larger extrapolation in  $m_t - m_0$

$K^+$	yield $\times 10^{-2}$ [1/ evt]	$T_{eff}$ [MeV]
0 - 40%	$3.01 \pm 0.03 \pm 0.15 \pm 0.30$	$104 \pm 1 \pm 1$
0 - 10%	$5.98 \pm 0.11 \pm 0.30 \pm 0.60$	$110 \pm 1 \pm 1$
10 - 20%	$3.39 \pm 0.05 \pm 0.17 \pm 0.34$	$103 \pm 1 \pm 1$
20 - 30%	$1.88 \pm 0.02 \pm 0.09 \pm 0.19$	$97 \pm 1 \pm 1$
30 - 40%	$1.20 \pm 0.02 \pm 0.06 \pm 0.12$	$91 \pm 1 \pm 1$
$K^-$	yield $\times 10^{-4}$ [1/evt]	$T_{eff}$ [MeV]
0 - 40%	$1.94 \pm 0.09 \pm 0.10 \pm 0.10$	$84 \pm 6$
0 - 20%	$3.36 \pm 0.31 \pm 0.17 \pm 0.17$	$84 \pm 7$
20 - 40%	$1.28 \pm 0.11 \pm 0.06 \pm 0.06$	$69 \pm 7$
$\phi$	yield $\times 10^{-4}$ [1/evt]	$T_{eff}$ [MeV]
0 - 40%	$0.99 \pm 0.24 \pm 0.10 \pm 0.05$	$108 \pm 7$
0 - 20%	$1.55 \pm 0.28 \pm 0.15 \pm 0.11$	$99 \pm 8$
20 - 40%	$0.53 \pm 0.08 \pm 0.05 \pm 0.04$	$91 \pm 7$
$K^-/K^+ \times 10^{-3}$		$\phi/K^-$
0 - 40%	$6.45 \pm 0.9$	$0.52 \pm 0.16$
0 - 20%	$7.17 \pm 1.1$	$0.46 \pm 0.12$
20 - 40%	$8.31 \pm 1.3$	$0.44 \pm 0.10$

TABLE I: Multiplicities and effective inverse slopes at mid-rapidity  $T_{eff}$  as well as multiplicity ratios for given centrality classes. The first given error corresponds to the statistical, the second to the systematic error within the rapidity range covered by HADES and the last one to the extrapolation uncertainty to full phase space. If the second or third error is not given, it is found to be well below the statistical error and is hence neglected. The error on the multiplicity ratios corresponds to the quadratic sum of the single error sources.

into account by an additional systematic error when extracting  $T_{eff}$  of the  $K^-$ .

The hierarchy in excess-energies discussed above is reflected in the yields of the three mesons.  $K^+$  mesons are found to be two orders of magnitude more abundantly produced than the deep sub-threshold produced  $K^-$  and  $\phi$  mesons. Due to the, already previously observed, similar rise of charged kaon yields with increasing centrality, we directly compare the extracted ratio  $K^-/K^+ = (6.45 \pm 0.77) \times 10^{-3}$  to values obtained by the KaoS collaboration at higher beam energies and various collision systems [12, 23], without correcting for the different centrality selections. The ratio shows a linear increase with  $\sqrt{s_{NN}}$ , see left side of Fig. 3. Our data point is consistent with the extrapolation from higher energies using a linear regression (displayed as the dotted line).

The yield and slope of the  $\phi$  meson have never been measured before in Au+Au collisions at SIS18 energies. We find a  $\phi/K^-$  ratio of  $0.52 \pm 0.16$ , hence resonant production is indeed a sizable source of  $K^-$ . The excitation function of the ratio is depicted on the right side of Fig. 3 as a function of  $\sqrt{s_{NN}}$ , including measurements nearby in energy in lighter systems [23–26], as well as data from higher energies [42, 43]. The ratio decreases with increasing energy, before it saturates at  $\approx 0.15$

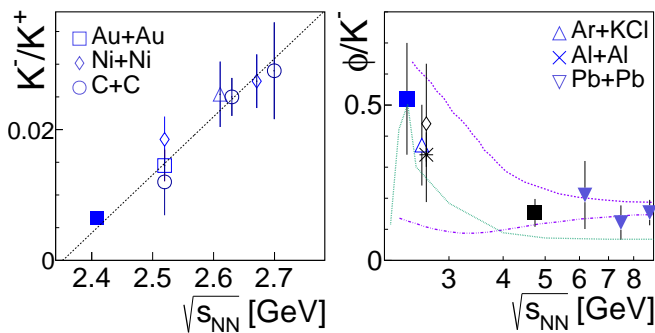


FIG. 3: Left: Multiplicity ratio  $K^-/K^+$  for various collision systems as function of  $\sqrt{s_{NN}}$  [12, 23] together with an extrapolation from higher energies, using a linear regression (displayed as the dashed curve). Right: Multiplicity ratio  $\phi/K^-$  as function of  $\sqrt{s_{NN}}$  [23–26, 42, 43]. Purple curves depict statistical model calculations using  $R_c$  values of 2.2 fm (dashed curve) and 4.2 fm (dashed dotted curve) [48, 49]. The green dotted curve corresponds to a tuned version of UrQMD [34].

for  $\sqrt{s_{NN}} \geq 5$  GeV. The rise of the ratio towards low energies is in conflict with the still widespread assumption of a small hadronic  $\phi$  cross section [28]. Along this line, recent data from elementary collisions [46] and investigations about the  $\phi$  meson self-energy in nuclear matter [47] show clear violations of the classic OZI rule.

This rise can be qualitatively reproduced by statistical model calculations when using the so-called strangeness correlation radius  $R_c$  as a canonical suppression parameter. As the  $\phi$  meson has no net-strangeness, it is not sensitive to strangeness conservation in the reduced volume and therefore not suppressed, while the  $K^-$  meson is. This results in the observed decrease of the  $\phi/K^-$  ratio with increasing  $\sqrt{s_{NN}}$ . In the right panel of Fig. 3, the displayed purple curves are based on the same parameterization of  $T$  and  $\mu_B$  but different values of  $R_c$  [48, 49]. The size of  $R_c$  determines the strength of the decrease. Whether the model is able to describe the data also quantitatively will be answered when more hadron yields become available and a fit including those yields can be performed. Also the transport code UrQMD [34] can describe the data for energies below 3 GeV, after being tuned to match data on elementary  $\phi$  production cross sections [36] using higher-lying baryonic resonances as energy reservoir quantitatively, displayed by the dotted green line on the right side of Fig. 3.

When comparing the  $\phi/K^-$  and the  $K^-/K^+$  ratios extracted within the two centrality classes one naively expects the relative yields to show different scaling with the system size as a different amount of energy for the production must be accumulated in multi-step processes. However, we find both ratios not to increase towards central events and hence not to reflect the hierarchy in production thresholds, see Tab.1. While the scaling of the  $K^-$  was previously explained by strangeness exchange, the similar increase of the  $\phi$  mesons is impos-

sible to explain by such reactions in a classical particle picture. This implies that the created system is much more coherent than generally assumed and suggests that the total amount of produced strangeness increases with decreasing impact parameter of the collision before it is redistributed to the different hadron species at freeze-out [44].

To investigate the effect of the  $\phi$  feed-down on the  $K^-$  spectra we built a simple two-component model using the event generator Pluto [45]. We use two static thermal sources, one for direct  $K^-$  and one for  $\phi$  mesons with temperatures of  $T = 104$  MeV and  $T = 108$  MeV according to the measured inverse slopes of the  $K^+$  and of the  $\phi$  meson. Due to the hierarchy in production yields the feed-down on the  $K^+$  spectra is negligible. In case of the  $K^-$ , we scale the two contributions of direct and resonantly produced  $K^-$  according to the measured  $\phi/K^-$  ratio. The resulting sum of both contributions is then fitted using Eq. (1) in a similar  $m_t - m_0$  range between 0 and 200 MeV/ $c^2$  as used for experimental data. The extracted inverse slopes for different  $K^-$  sources are displayed on the right panel in Fig. 2: direct thermal (blue), resulting from  $\phi$  decays (red), sum of both (green). The inverse slope of  $(86 \pm 2)$  MeV agrees with the measurement of  $K^-$  of  $(84 \pm 6)$  MeV. The error is obtained by variation of the  $\phi/K^-$  ratio within the given errors. The error on the inverse slope parameter of the experimental spectrum is propagated by making use of the covariance matrix when determining the yields and hence is not varied explicitly. We find the shape of the rapidity distribution to be reproduced as well, displayed together with the  $K^-$  data on the left panel of Fig. 2, where a comparison of the data to the two-component model (green curve), the direct (blue curve) and contribution from  $\phi$  decays (red curve) is shown. According to Occam's razor, the simplest assumption should be used to explain the different slopes. This implies, that a prominent indication for sequential freeze-out of kaons and antikaons is obsolete. In summary, we have presented first data on charged kaons and  $\phi$  mesons in Au+Au collisions at  $\sqrt{s_{NN}} = 2.4$  GeV. We find the observed yield ratios and slopes of charged kaons to agree well with observations at slightly higher energies. The  $\phi/K^-$  ratio is found to be  $0.52 \pm 0.16$ . Hence, production via  $\phi$  mesons turns out to be a sizable source of antikaon production. The ratio shows a decrease with increasing center-of-mass energy  $\sqrt{s}$ , which is in strong conflict with the picture of a small hadronic  $\phi$  cross section [28]. The  $\phi/K^-$  ratio is constant as function of centrality, suggesting a universal scaling of produced strangeness with increasing system size. The different slopes of the  $K^+$  and  $K^-$  spectra can be fully explained by feed-down of  $\phi$  mesons. As a direct consequence, attempts to extract the  $K^-$ -N potential and all further conclusions based on it e.g. for astrophysical objects or general properties of QCD matter are misleading and need to be revisited.

The HADES collaboration gratefully acknowl-

edges the support by the grants SIP JUC Cracow (Poland), 2013/10/M/ST2/00042; TU Darmstadt (Germany), VH-NG-823; GU Frankfurt, (Germany), BMBF:05P15RFFCA, HIC for FAIR, ExtreMe Matter Institute EMMI; TU München, Garching (Germany),

MLL München, DFG EClust 153, DFG FAB898/2-1, BmBF 05P15WOFCA; JLU Giessen (Germany), BMBF:05P12RGGHM; IPN, N2P3/CNRS N2P3/CNRS (France); NPI CAS Rez (Czech Republic), GACR 13-06759S, MSMT LM2015049.

- 
- [1] D. B. Kaplan and A. E. Nelson, Phys. Lett. B **175** (1986) 57.
  - [2] C. H. Lee, G. E. Brown, D. P. Min and M. Rho, Nucl. Phys. A **585** (1995) 401.
  - [3] J. Schaffner-Bielich, J. Bondorf, A. Mishustin, Nucl. Phys. A **625**, (1997) 325.
  - [4] M. F. M. Lutz, A. Steiner and W. Weise, Nucl. Phys. A **574** (1994) 755.
  - [5] V. Koch, Phys. Lett. B **337** (1994) 7.
  - [6] W. Cassing, E. L. Bratkovskaya, U. Mosel, S. Teis, A. Sibirtsev, Nucl. Phys. A **614** (1997) 415.
  - [7] D. Cabrera, L. Tolos, J. Aichelin and E. Bratkovskaya, J. Phys. Conf. Ser. **668** (2016) 012048.
  - [8] V.K.Magas et al. Phys.Rev.Lett. **95** (2005) 052301.
  - [9] G. Agakishiev *et al.* [HADES Collaboration], Phys. Rev. C **87** (2013) 025201.
  - [10] F. Laue *et al.* [KaoS Collaboration], Phys. Rev. Lett. **82** (1999) 1640.
  - [11] M. Menzel *et al.* [KaoS Collaboration], Phys. Lett. B **495** (2000) 26.
  - [12] A. Förster, F. Uhlig, I. Bottcher, D. Brill, M. Debowski *et al.*, Phys. Rev. C **75** (2007) 024906.
  - [13] C. M. Ko, Phys. Lett. B **120** (1983) 294.
  - [14] C. Hartnack, H. Oeschler and J. Aichelin, Phys. Rev. Lett. **90** (2003) 102302.
  - [15] W. Cassing, L. Tolos, E. L. Bratkovskaya and A. Ramos, Nucl. Phys. A **727** (2003) 59.
  - [16] C. Fuchs, Prog. Part. Nucl. Phys. **56** (2006) 1
  - [17] C. Hartnack, H. Oeschler, Y. Leifels, E. L. Bratkovskaya, J. Aichelin, Phys. Rept. **510** (2012) 119.
  - [18] G. E. Brown and H. Bethe, Astrophys. J. **423** (1994) 659.
  - [19] G. Q. Li, C. H. Lee and G. E. Brown, Phys. Rev. Lett. **79** (1997) 5214.
  - [20] P. Demorest *et al.*, Nature **476**, (2010) 1081.
  - [21] J. Antoniadis *et al.*, Science **340**, (2013) 6131.
  - [22] A. Mangiarotti *et al.* [FOPI Collaboration], Nucl. Phys. A **714** (2003) 89.
  - [23] G. Agakishiev *et al.* [HADES Collaboration], Phys. Rev. C **80** (2009) 025209.
  - [24] K. Piasecki *et al.* [FOPI Collaboration], Phys. Rev. C **91**, (2015) 054904.
  - [25] P. Gasik *et al.* [FOPI Collaboration], Eur. Phys. J. A **52** (2016) 177.
  - [26] K. Piasecki *et al.* [FOPI Collaboration], Phys. Rev. C **94** (2016) 014901.
  - [27] S. Okubo, Phys. Lett. 5 (1963) 1975; G. Zweig, CERN Report (1964) No.8419/TH412; J. Iizuka, Prog. Theor. Phys. Suppl. 37, (1966) 38.
  - [28] A. Shor, Phys. Rev. Lett. **54** (1985) 1122.
  - [29] W. S. Chung, G. Q. Li and C. M. Ko, Nucl. Phys. A **625** (1997) 347.
  - [30] B. Kämpfer, R. Kotte, C. Hartnack, J. Aichelin, J. Phys. G **28** (2002) 2035.
  - [31] G. Agakishiev *et al.* [HADES Collaboration], Eur. Phys. J. A **47** (2011) 21.
  - [32] G. Agakishiev *et al.* [HADES Collaboration], Phys. Rev. C **93** (2016), 064908.
  - [33] H. Schade, G. Wolf and B. Kämpfer, Phys. Rev. C **81** (2010) 034902.
  - [34] J. Steinheimer and M. Bleicher, J. Phys. G **43** (2016) 015104.
  - [35] M. Lorenz *et al.* [HADES Collaboration], PoS (BORMIO2010) (2010) 038.
  - [36] Y. Maeda *et al.* [ANKE Collaboration], Phys. Rev. C **77** (2008) 015204.
  - [37] G. Agakishiev *et al.* [HADES Collaboration], Eur. Phys. J. A **41** (2009) 243.
  - [38] R. J. Glauber and G. Matthiae, Nucl. Phys. B **21** (1970) 135.
  - [39] B. Kardan, Diploma Thesis, Goethe-University Frankfurt (2016); G. Agakishiev *et al.* [HADES Collaboration] manuscript in preparation,
  - [40] S. A. Bass *et al.*, Prog. Part. Nucl. Phys. **41** (1998) 225.
  - [41] H. Schuldes, PhD Thesis, Goethe-University Frankfurt (2016).
  - [42] B. Holzman *et al.* (E917), Nucl. Phys. A 698 (2002) 643.
  - [43] S. V. Afanasiev *et al.* (NA49), Phys. Lett. B 491 (2000) 59.
  - [44] E. E. Kolomeitsev, B. Tomasik and D. N. Voskresensky, Phys. Rev. C **86** (2012) 054909.
  - [45] I. Fröhlich *et al.*, J.Phys. Conf. Ser. 219 (2010) 032089.
  - [46] T. Ishikawa *et al.*, Phys. Lett. B 608 (2005) 215; M. Hartmann *et al.*, Phys. Rev. Lett. 96 (2006) 242301; F. Balestra *et al.*, Phys. Rev. C **63** (2001) 024004. A. Sibirtsev and W. Cassing, Eur. Phys. J. A 7, (2000) 407.
  - [47] D. Cabrera, A. N. Hiller Blin and M. J. Vicente Vacas, Phys. Rev. C **95** (2017), 015201.
  - [48] J. Cleymans, H. Oeschler, K. Redlich and S. Wheaton, Phys. Rev. C **73** (2006) 034905.
  - [49] K. Redlich, private communication.